

Geometrical Defects in Josephson Junction Arrays

Kieran Mullen

University of Oklahoma, Department of Physics, Norman, OK 73019-0225

Abstract

Dislocations and disclinations in a lattice of Josephson junctions will affect the dynamics of vortex excitations within the array. These defects effectively distort the space in which the excitations move and interact. We calculate the interaction energy between such defects and excitations, determine vortex trajectories in twisted lattices, and discuss the consequences for experiment.

I. INTRODUCTION

A host of interesting experiments have already been performed on regular arrays of Josephson junctions. Tuning the ratio of the pair charging energy to the Josephson coupling energy in such experiments allows one to pass from a regime where the dynamics is dominated by vortex excitations, to one where it is dominated by charge soliton excitations.¹ In the vortex dominated regime one can examine such issues as the ballistic propagation of vortices,^{2,3} the Kosterlitz-Thouless (KT) vortex unbinding transition,^{4–6} and how the interference of vortices is influenced by electric charges in the Aharonov-Casher effect.⁷ In the charge dominated regime the parallel issues of the propagation of solitons,^{8,9} the possibility of the KT charge unbinding transition⁹ and how the interference of charges is influenced by magnetic fields in the Aharonov-Bohm effect^{10,11} have been investigated. The charges and vortices in a superconductor are approximately dual, and the physics of the two reflect this symmetry.^{12,13}

In this paper we study the motion of vortices in arrays that possess topological defects. Studies of Josephson junction arrays usually focus on either square or triangular lattices, where the structure is uniform. It is an unspoken assumption that the lattice of junctions be free from *spatial* defects such as dislocations (*e.g.* a missing line of junctions as in fig.(1.a) or disclinations (*e.g.* a missing wedge of junctions, as in fig.(1.b)). We focus on the regime where E_J , is larger or on the order of E_C , so that vortices can be viewed as stable massive particles with a mass determined by their charging energy. Under these conditions vortices are free to move ballistically in the array. We find that the defects act as distortions in the 2D world in which the excitations move, with two effects. First, “straight lines” (geodesics) in this twisted coordinate system differ from those in Cartesian coordinates, and second the fields surrounding the excitations are perturbed by the twisted geometry, altering the interaction between vortices and leading to an interaction between vortices and the geometrical defects.

The fundamental origin of the interaction between vortices and topological defects is not

hard to see. The self-energy of the vortex depends upon spatial gradients in the superconducting phase. Dislocations and disclinations involve either the removal or insertion of extra junctions in the pristine lattice. From the point of view of the vortices this means there are either missing or added regions of space in the two dimensional plane. This affects the gradients and thus the self energy.

In section II below we develop a continuum description of the dynamics on a distorted lattice. We then analyze the effect of topological irregularities on the dynamics of a single vortex in an array in which $E_J \geq E_C$, i.e., an array in which a vortex can be viewed as a stable massive particle. In section III we calculate the interaction of vortices or charges on the twisted lattice. We use these results in section IV to calculate the motion of vortices in a lattice with defects. The effects of the defects should be observable in experiments in which the ballistic motion of vortices is probed. We conclude in section V.

In the calculations below we use Einstein summation notation in which we sum over repeated indices. Roman indices range over the values 1 and 2, greek indices for the 2+1 dimensional space-time range over 0, 1 and 2. Bold face variables are 2-vectors; hatted vectors are normalized.

II. DEVELOPMENT OF THE CONTINUUM DESCRIPTION

We consider an array of Josephson junctions in an externally applied magnetic field perpendicular to the array. We assume that the array has only smooth distortions in its structure, and a small number of defects such as the dislocation or disclination in fig.1. Arrays of Josephson junctions are customarily described in terms of the set of variables φ_a , and n_a , the phase of the super-conducting order parameter and the number of excess Cooper pairs on super-conducting island a . Although the islands themselves are extended objects, we consider the phase and charge as being defined at a discrete set of points. (That is, we require the island width to be smaller than or on the order of the correlation length, so that the phase across the island is a constant). The thermodynamics of the array is derivable

from a Hamiltonian made out of two contributions, the Coulomb charging energy and the Josephson coupling energy. The partition function can be written as a path integral over the charge and phase degrees of freedom:

$$\mathcal{Z} = \sum_{n_a} \int \mathcal{D}\varphi_a \exp \left\{ -\frac{1}{\hbar} S[n_a, \varphi_a] \right\} \quad (1)$$

with the action given by,

$$S[n_a, \varphi_a] = \int_0^\beta d\tau \left[-i\hbar n_a \dot{\varphi}_a - 2e^2 n_a n_b C_{ab}^{-1} + \sum'_{a,b} E_j (1 - \cos(\varphi_a - \varphi_b - \theta_{ab})) \right] \quad (2)$$

where repeated indices are summed and the path integral in τ is computed in the standard step-wise fashion. The quantity $C_{a,b}^{-1}$ is an element of the inverse capacitance matrix element between islands a and b , E_J is the Josephson coupling energy between two nearest neighbor junctions, and $\beta = 1/k_B T$ where T is the temperature and k_B is Boltzman's constant. The primed sum indicates that only nearest-neighbor phase differences are included. The phase difference θ_{ab} is caused by the externally applied magnetic field and is determined from the \mathbf{A} , the magnetic vector potential, via

$$\theta_{ab} \equiv \int_a^b \mathbf{A}(\mathbf{x}) \cdot d\mathbf{x}. \quad (3)$$

where we have absorbed a factor of $2e/c$ into $\mathbf{A}(\mathbf{x})$

We next make the standard Villain approximation to decompactify the phase.¹⁴ We introduce a set integer variables, $v_a^{(0)}$ defined on each island, and v_{ab} , associated with each nearest-neighbor pair of islands and approximate eq.(2) as:

$$Z \approx c_0 \int \mathcal{D}n_a \int \mathcal{D}\varphi_a \sum_{v_{ab}, v_a^{(0)}} \exp \left\{ -\frac{1}{\hbar} \int_0^\beta \left[-in_a(\hbar\dot{\varphi}_a + 2\pi v_a^{(0)}) - 2e^2 n_a n_b C_{ab}^{-1} \right. \right. \\ \left. \left. + \sum'_{a,b} \frac{E_j}{2\hbar} (\varphi_a - \varphi_b - \theta_{ab} + 2\pi v_{ab})^2 \right] \right\} \quad (4)$$

where c_0 is a constant prefactor whose value depends upon E_J and the capacitance. The variable n_a is now continuous; by summing over $v_a^{(0)}$ we recover only its integer contributions. Following the Villain transformation, the phase φ_{ab} are all regular (*i.e.* non-compact) variables. The vorticity is all contained in the variables v_{ab} .

The system described by eq(2), or eq(4), is evaluated on a lattice of points, a lattice that may possess topological defects such as dislocations or disclinations. As in the case of a regular lattice, the long wavelength low frequency properties are obtained from a continuum description of the lattice.^{15,13} In the case of a distorted lattice, however, the continuum description should reflect the lattice distortions. Our goal is the construction of a continuum Lagrangian whose long wave length low frequency properties are the same as those of the discrete model of eq(4).

Although the phase φ_a is only defined at a discrete set of points, we may define a continuous function $\varphi(\mathbf{x})$ which smoothly interpolates between the phases defined at each lattice point. We replace the phase difference between two islands by a Taylor expansion:

$$\begin{aligned} \varphi_a - \varphi_b &= \varphi(\mathbf{x}_a) - \varphi(\mathbf{x}_b) \\ &\approx \nabla \varphi(\mathbf{x}_a) \cdot \mathbf{u}_{(i)}(\mathbf{x}_a) \end{aligned} \quad (5)$$

where $\mathbf{u}_{(i)}(\mathbf{x}_a)$ is a vector connecting two adjacent islands. There will be two such vectors ($i = 1, 2$) associated with each island, as shown in fig.2. The direction and length of the vectors will change as we move through the distorted lattice. In a similar fashion we associate a pair of the integers, v_{ab} and $v_{ab'}$ with these directions so that $\mathbf{v}_{(1)}(\mathbf{x}_a) = v_{ab} \hat{\mathbf{u}}_{(1)}(\mathbf{x}_a) / u_{(1)}(\mathbf{x}_a)$ and $\mathbf{v}_{(2)}(\mathbf{x}_a) = v_{ab'} \hat{\mathbf{u}}_{(2)}(\mathbf{x}_a) / u_{(2)}(\mathbf{x}_a)$ where $u_{(i)}(\mathbf{x}_a) \equiv |\mathbf{u}_{(i)}(\mathbf{x}_a)|$, and $\hat{\mathbf{u}}_{(i)}(\mathbf{x}_a) \equiv \mathbf{u}_{(i)}(\mathbf{x}_a) / u_{(i)}(\mathbf{x}_a)$

Similarly, we approximate the contribution from the magnetic field by:

$$\theta_{ab} \approx \mathbf{A}(\mathbf{x}_a) \cdot \mathbf{u}_{(1)}(\mathbf{x}_a) \quad \theta_{ab'} \approx \mathbf{A}(\mathbf{x}_a) \cdot \mathbf{u}_{(2)}(\mathbf{x}_a) \quad (6)$$

so that our partition function becomes

$$\begin{aligned} Z \approx c_0 \int \mathcal{D}n(\mathbf{x}_a) \int \mathcal{D}\varphi(\mathbf{x}_a) \sum_{\mathbf{v}_{(i)}(\mathbf{x}_a), v^{(0)}(\mathbf{x}_a)} \exp \left\{ -\frac{1}{\hbar} \int_0^\beta \left[-i n(\mathbf{x}_a) (\dot{\varphi}(\mathbf{x}_a) + 2\pi v_a^{(0)}) - \right. \right. \\ \left. \left. 2e^2 n(\mathbf{x}_a) n(\mathbf{x}_b) C_{\mathbf{x}_a, \mathbf{x}_b}^{-1} + \sum_a \sum_{i=1,2} \frac{E_j}{2\hbar} \left[(\partial_k \varphi(\mathbf{x}_a) - A_k(\mathbf{x}_a) + 2\pi v_{(i)}^k(\mathbf{x})) u_{(i)}^k(\mathbf{x}) \right]^2 \right] \right\} \end{aligned} \quad (7)$$

We would like to turn this discrete sum over the lattice points \mathbf{x}_a and nearest neighbor vectors $\mathbf{u}_{(i)}(\mathbf{x})$ into an integral over the Cartesian coordinates x_1 and x_2 in the plane.

All geometrical information about the lattice is contained within the vectors $\mathbf{u}_{(i)}(\mathbf{x})$, since they indicate the direction and distance to the nearest neighbors. Locally each of the $\mathbf{u}_{(i)}(\mathbf{x})$ can be written as

$$\mathbf{u}_{(i)} = \left(a_{(1)}^i \hat{\mathbf{e}}_1 + a_{(2)}^i \hat{\mathbf{e}}_2 \right) \quad (8)$$

where we have suppressed the spatial dependence and the $\hat{\mathbf{e}}_i$ are the Cartesian unit vectors. We note that the $a_{(j)}^i$ are the 2D analogs of basis triads in differential geometry; they relate differentials in the local, twisted reference frame (the $\mathbf{u}_{(i)}$) to the Cartesian frame.¹⁶ We may rewrite gradient-squared terms as:

$$\sum_{i=1,2} \left(\nabla \varphi \cdot \mathbf{u}_{(i)} \right)^2 = \partial_j \varphi \partial_k \varphi a_i^j a_i^k \quad (9)$$

We introduce the matrix $g^{jk} \equiv a_i^j a_i^k$; its inverse, denoted by g_{jk} , is the *metric tensor*. A small displacement in the Cartesian coordinates, $d\mathbf{x} = dx^1 \hat{\mathbf{e}}_1 + dx^2 \hat{\mathbf{e}}_2$, has a distance when measured in the number of junction interfaces crossed (or dimensionless junction “hops”) of

$$ds^2 = g_{jk} dx^j dx^k \quad (10)$$

whence the name “metric”.

Furthermore, the area a of the plaquet bounded by $\mathbf{u}_{(1)}$ and $\mathbf{u}_{(2)}$ is just

$$\mathcal{A} = |\mathbf{u}_{(1)} \times \mathbf{u}_{(2)}| \quad (11)$$

$$= \sqrt{\det g_{ij}} u_{(1)} u_{(2)} \quad (12)$$

$$\equiv g^{1/2} u_{(1)} u_{(2)} \quad (13)$$

Note that the metric tensor and its determinant may vary in space.

We must also convert the capacitance terms to a continuum form. The original capacitance matrix satisfies $Q_a = C_{ab}V_b$ where V_b is voltage on island b ; if we assume only nearest neighbor coupling, then this can be written as:¹³

$$(4C_1 + C_0)V_a - C_1 \sum_{\text{neighbors}} V_b = 2e n_a \quad (14)$$

where the sites b are neighbors of a . The variables C_0 and C_1 are the diagonal and off-diagonal elements of the capacitance matrix. If we neglect the diagonal self-capacitance, ($C_0 = 0$), it states that the discrete divergence of V equals the charge on a given island. Through an analysis similar to what was done for the phase, we can define a continuous field $V(\mathbf{x})$ and replace the above discrete equation by

$$(C_1 g^{-1/2} \partial_i g^{1/2} g^{ij} \partial_j + \tilde{C}_0(\mathbf{x})) V(\mathbf{x}) = 2e n(\mathbf{x}) \quad (15)$$

where $n(\mathbf{x})$ consists of a sum of δ -functions, and $\tilde{C}_0(\mathbf{x})$ is a capacitance density given by C_0/a . If we neglect this self-capacitance term, then the left hand side is the Laplace-Beltrami (LB) operator, and the inverse capacitance matrix is equivalent the Green function of this differential operator in the appropriate continuum limit. Let us denote this Green function by $C^{-1}(\mathbf{x}, \mathbf{x}')$ and define $U(\mathbf{x}, \mathbf{x}') = \lim_{C_0 \rightarrow 0} C^{-1}(\mathbf{x}, \mathbf{x}')$. In a flat space $C^{-1}(\mathbf{x}, \mathbf{x}') = K_0(2e\sqrt{C_1/\tilde{C}_0} |\mathbf{x} - \mathbf{x}'|)$ where $K_0(x)$ is the zero order Bessel function of imaginary argument, and $U(\mathbf{x}, \mathbf{x}') = (2\pi C_1)^{-1} \log |\mathbf{x} - \mathbf{x}'|$.¹⁶

If we take the continuum limit where a becomes an infinitesimal then we can replace the sums by integrals over area and write the action as:

$$\begin{aligned} S[n(\mathbf{x}), \varphi(\mathbf{x})] = & -\frac{1}{\hbar} \int_0^\beta \int d\mathbf{x} g^{1/2}(\mathbf{x}) \left[-i n(\mathbf{x}) (\dot{\varphi}(\mathbf{x}) + 2\pi v^{(0)}(\mathbf{x})) - \right. \\ & + \frac{E_j}{2\hbar} (\partial_j \varphi(\mathbf{x}) - A_j(\mathbf{x}) + 2\pi v_{(i)}^j(\mathbf{x})) (\partial_k \varphi(\mathbf{x}) - A_k(\mathbf{x}) + 2\pi v_{(i)}^k(\mathbf{x})) g^{jk} \\ & \left. 2e^2 \int d\mathbf{x}' g^{1/2}(\mathbf{x}') n(\mathbf{x}) n(\mathbf{x}') C^{-1}(\mathbf{x}, \mathbf{x}') \right] \end{aligned} \quad (16)$$

where $n(\mathbf{x}_a)$ is the charge density.

We now wish to perform a series of operations on the action so as to bring the vortex degrees of freedom to the fore. These steps are standard ones for deriving the interactions of vortices in 2D systems, made slightly more tedious by the necessity to keep track of the local metric. While they appear messy and involved, one should keep in mind that these steps are identical to what one would do if we had a regular, uniform array, but wished to evaluate all quantities in curvilinear (*i.e.* polar) coordinates. Furthermore, if we choose our

lattice to be smooth and undistorted, so that $g_{ij} = \delta_{ij}$, we should regain the standard vortex interaction.

We first decouple the Josephson term via a Hubbard-Stratonovich transformation, introducing a new field $\mathbf{p}(\mathbf{x})$. The second term then becomes:

$$\int d\mathbf{x} g^{1/2} \left[\frac{1}{2E_j} p_i p_j g^{jk} + (\partial_k \varphi - A_k + 2\pi v_{(i)}^k) p_j g^{jk} \right] \quad (17)$$

The action is now linear in φ ; integrating it out we obtain the constraint:

$$\dot{n}(\mathbf{x}) = -g^{-1/2} \partial_k g^{1/2} g^{jk} p_j \quad (18)$$

The right hand side is just the divergence of \mathbf{p} expressed in invariant form. In order to satisfy this constraint we first express it in a “space-time” notation, using greek indices $\mu \in \{0, 1, 2\}$, setting $\partial_0 = \partial_t$ and defining the 3-momentum $p_\mu = (n(\mathbf{x}), p_1(\mathbf{x}), p_2(\mathbf{x}))$. Then eq.(18) can be rewritten

$$g^{\mu\nu} D_\mu p_\nu = 0 \quad (19)$$

where $g_{\mu\nu}$ is the the 3x3 metric,

$$g_{\mu\nu} \equiv \begin{pmatrix} 1 & 0 \\ 0 & g_{ij} \end{pmatrix} \quad (20)$$

and D_μ is the covariant derivative. Note that trivially $\det g_{\mu\nu} = \det g_{ij}$. Eq.(19) can be satisfied if p_μ is the covariant curl of a vector field:

$$\epsilon^{\kappa\lambda\mu} g_{\nu\kappa} D_\lambda K_\mu = 2\pi p_\nu \quad (21)$$

where K_μ is an auxiliary or gauge field and $\epsilon^{\kappa\lambda\mu}$ is the totally antisymmetric Levi-Civita tensor. Since covariant derivatives of the metric are zero, eq.(19) is satisfied automatically. We rewrite our action in terms of the gauge fields K_μ , expressing $n(\mathbf{x})$ and $\mathbf{p}(\mathbf{x})$ using eq.(21) As is common with such fields, we may choose a gauge condition for K_μ that will simplify the algebra: we choose

$$g^{ij} D_i K_j = 0 \quad (22)$$

in which case we the action becomes:

$$S[K_\mu] = -\frac{1}{\hbar} \int d\tau \int d\mathbf{x} g^{1/2}(\mathbf{x}) \left[i\epsilon^{\mu\nu\lambda} (v_\lambda D_\mu K_\nu - A_\lambda D_\mu K_\nu) + \frac{1}{8\pi^2 E_J} (\partial_i K_0 \partial_j K_0 + \partial_0 K_i \partial_0 K_j) g^{ij} + \frac{e^2}{2\pi^2 C_1} \int d\mathbf{x}' g^{1/2}(\mathbf{x}') \epsilon_{ij} \epsilon_{kl} D_i K_j(\mathbf{x}) D_k K_\ell(\mathbf{x}') C^{-1}(\mathbf{x}, \mathbf{x}') \right] \quad (23)$$

where $A_\mu = (0, A_1, A_2)$. Integrating by parts on the first term we obtain

$$S[K_\mu] = -\frac{1}{\hbar} \int d\tau \int d\mathbf{x} g^{1/2}(\mathbf{x}) \left[ig^{\mu\nu} (J_\nu - \Phi_\nu) K_\mu + \frac{1}{2E_J} g^{ij} (\partial_i K_0 \partial_j K_0 + \partial_0 K_i \partial_0 K_j) + \int d\mathbf{x}' g^{1/2}(\mathbf{x}') \epsilon_{ij} \epsilon_{kl} D_i K_j(\mathbf{x}) D_k K_\ell(\mathbf{x}') C^{-1}(\mathbf{x}, \mathbf{x}') \right] \quad (24)$$

where Φ is a magnetic field density, $\Phi_\mu = (B_z/\Phi_0, 0, 0)$, and J_ν is a vortex current density related to our field \mathbf{v} by a covariant curl:¹⁵

$$J^\lambda = \epsilon^{\lambda\mu\nu} D_\mu v_\nu \quad (25)$$

This is the continuum version of the distorted Josephson junction lattice. The K_μ field mediates the interaction between vortex charges and currents. The action is quadratic in these fields, and thus the path integrals over K_μ can be performed. The resulting action will give the vortex Hamiltonian in the curved space. This is done in section III below.

III. VORTEX INTERACTIONS IN A CURVED SPACE

The continuum action of eq.(24) is expressed in terms of the gauge fields and the vortices. We would like to integrate out the K_μ so as to have an action solely in terms of the vortex degrees of freedom. First, we write the vortex current density as a sum over discrete point vortices located at positions $\mathbf{X}^{(n)}$:

$$J_\nu = \sum_n \rho(\mathbf{X}^{(n)}(t)) \delta(\mathbf{x} - \mathbf{X}^{(n)}(t)) \left(1, \dot{X}_1^{(n)}(t), \dot{X}_2^{(n)}(t) \right) \quad (26)$$

where $\rho(\mathbf{X}^{(n)})$ is the charge of the vortex located at $\mathbf{X}^{(n)}$.

We can integrate out the K_0 field as follows: integration by parts on the quadratic term yields $K_0 g^{-1/2} \partial_i g^{1/2} g^{ij} \partial_j K_0$; this combination of metrics and derivatives is just the LB operator, the generalization of the Laplacian to this curved space. Integrating out K_0 will yield a potential interaction between vortices, $U(\mathbf{x}, \mathbf{x}')$.

We next examine the K_i dependence. The $\partial_t K_i$ terms correspond to a retarded interaction between the vortices; we can neglect this non-locality in time so long as the characteristic velocity of vortices is much less than $\omega_j \ell$, where $\omega_j = \sqrt{8E_J E_C}/\hbar$, and ℓ is a characteristic island size.¹³ Doing so amounts to making the charge and vortex degrees of freedom exactly dual. We further assume that C_0 is small and we can approximate the inverse capacitance kernel with $U(\mathbf{x}, \mathbf{x}')$. As discussed above, $U(\mathbf{x}, \mathbf{x}')$ is the inverse of the LB operator; when we perform the path integral it must cancel out the powers of ∇ acting on K_i . This integration will generate two types of terms quadratic in the vortex velocities. The first will be self-interaction terms that generate a mass for the vortex; the second terms are a velocity dependent interaction between the vortices.¹³ Our final action then depends only on the vortex degrees of freedom

Putting this all together we get:

$$S_{\text{eff}} = \frac{1}{\hbar} \int d\tau \frac{1}{2} m_{\text{eff}} \sum_n g_{ij} \dot{X}_i^{(n)} \dot{X}_j^{(n)} + \frac{1}{2} \sum_{m,n} g_{ij} \dot{X}_i^{(m)} \dot{X}_j^{(n)} U(\mathbf{X}^{(m)}, \mathbf{X}^{(n)}) + \frac{1}{2} \sum_{m,n} \rho(\mathbf{X}^{(m)}) \rho(\mathbf{X}^{(n)}) U(\mathbf{X}^{(m)}, \mathbf{X}^{(n)}) \quad (27)$$

where $m_{\text{eff}} = \pi^2 \hbar^2 C_1 / 2e^2$ and we have suppressed the explicit dependence on time. The first term is the kinetic energy of the vortex in the twisted space; the second term is the velocity dependent vortex-vortex interaction, and the third is vortex-vortex potential.

In order to demonstrate the effect of the defects, we calculate the interaction kernel $U(x, x')$ for two simple cases, that of the disclination and the dislocation. In order to do so, we are simply solving for how point charges interact in the 2D curved space defined by the distorted lattice. In flat space the field about a point charge falls off logarithmically. If we set $z_1 = x + iy$, the 2D potential of a point charge located at Z in a *flat* plane can be

written as:

$$V(x, y) = V(z) = \frac{1}{2\pi} \operatorname{Re} q \ln(z - Z). \quad (28)$$

We will need this formulation below. The interaction energy for a set of charges in flat space is then:

$$E_{\text{flat}} = \frac{1}{4\pi} \sum_{i,j} \rho(\mathbf{X}^{(i)}) \rho(\mathbf{X}^{(j)}) \log |\mathbf{X}^{(i)} - \mathbf{X}^{(j)}| \quad (29)$$

In this result we have neglected a constant self-energy term for the vortices that diverges as the log of the system size. This term either forces the net vorticity of the system to be zero, or is compensated by the externally applied field.

Although this is a continuum model for a problem on a lattice, it is known that this Green function is well approximated by that of the continuum problem.¹⁹ This gives us confidence in similar approximations we make when we examine lattices with defects.

A. Disclinations:

A negative disclination (fig(1b)) in 2D can be viewed as the projection of a cone into the plane. In order to form the cone, a wedge of sites is removed from the lattice. Next, the exposed edges are brought together, puckering the surface into a cone. Finally, the lattice is projected from the 3D cone back down to a 2D plane. This final distortion or stretching of the lattice is irrelevant from the point of view of the excitations, since it does not change the number or connectivity of the junctions. We can thus approximate the interaction energy of a charge or vortex excitation with a negative disclination by calculating their energy on a cone, or equivalently, on a plane with a wedge removed (fig. 3). We therefore need only solve the Poisson equation for a single point charge on a cone in order to obtain the potential $U(\mathbf{x}, \mathbf{x}')$.

This problem on a cone is equivalent to a 2D electrostatics problem of a single point charge on the planar surface with a missing wedge, as depicted in fig. 3. The boundary

condition across the cut is that the electric field is continuous. We are free to choose our cut in any direction; we choose to place our charge on the positive x-axis and center the cut out wedge along the negative x-axis. The boundary condition now simplifies to the requirement that the normal component of the field is zero on the edges of the wedge, and the parallel component is continuous. We can achieve this by a simple conformal mapping.²⁰ We can open a wedge in the plane via the mapping $z \rightarrow z' = z^{1/p}$ For a wedge with an opening angle α (fig. 3) we require $p = 2\pi/(2\pi - \alpha)$. Then

$$V(z) = \operatorname{Re} \ln(z^p - Z^p) \quad (30)$$

From this result we can obtain the vortex-vortex interaction energy. In addition, the self-energy term generates an interaction energy between the charge and the disclination. This can be found by calculating the electric field near the charge, subtracting the part due to the self-interaction, and integrating the force on the charge to get an effective potential. Putting the two together we find that the interaction energy of a set of vortices (or charges) on a lattice with a disclination at the origin is:

$$E_{\text{disc}} = \frac{1}{4\pi} \left\{ \sum_{i,j} \rho(\mathbf{X}^{(i)}) \rho(\mathbf{X}^{(j)}) \right. \\ \left. \log \left[|\mathbf{X}^{(i)}|^{2p} + |\mathbf{X}^{(j)}|^{2p} - 2|\mathbf{X}^{(i)}|^p |\mathbf{X}^{(j)}|^p \cos p(\gamma_i - \gamma_j) \right] + \right. \\ \left. \sum_i \rho(\mathbf{X}^{(i)})^2 (p-1) \ln X^{(i)} \right\} \quad (31)$$

with $\gamma \equiv \arctan(X_2/X_1)$. Eq. 31 reduces to the correct result for $p = 1$ (no distortion) and $p = 2$ (a half plane with an image charge at $-z_0$). Translation invariance is explicitly broken by the defect.

We can see intuitively why such the electrostatic charge interacts with the defects by considering the density of field lines. Imagine a series of concentric circles drawn about the point charge. If a given circle does not intersect the wedge, then the circumference of the circle of radius R will be $2\pi R$. Once the circle intersects the tip of the wedge (or the apex of the cone, if we think in 3D), the circumference of the circle will be *smaller* than $2\pi R$, and the density of field lines radiating outward will be slightly higher. Thus the electrostatic

energy of the charge is lowered by moving in farther away from the tip of the cone. The reverse applies to a positive disclination, which allows the field to less dense, so that the electrostatic charge is attracted to the defect. This effect will not affect the vortex-vortex (or charge-charge) interaction if the particles are much closer to each other than they are to the disclination, ($|\mathbf{X}^{(i)} - \mathbf{X}^{(j)}| \ll |\mathbf{X}^{(i)}|, |\mathbf{X}^{(j)}|$)

The vortex-vortex interactions are altered by the presence of the defect, introducing terms where the topological “charge” is coupled to two such excitations. However, we do not find that three body interactions are introduced among the vortices themselves.

B. Dislocations:

A similar calculation can be performed for a dislocation of Burger’s vector \mathbf{b} which we choose to be located at the origin and corresponding to an additional row of junctions along the negative x-axis, $\mathbf{b} = b \hat{\mathbf{e}}_2$ as in fig.(1.a). In this case it is easiest to start with the solution for an infinite half-plane, setting $p = 2$ in eq(30). We then deform the half plane into an semi-infinite slot of width b extending along the positive x-axis using the general Schwarz transformation.²⁰ The resulting exact mapping is not invertible in a closed form; we approximate it with:

$$z \rightarrow z + \frac{b}{2\pi} \ln z \quad (32)$$

where we take $|\arg z| < \pi$. This result is asymptotically correct for $|\mathbf{b}| \ll |\mathbf{r}|$, but lacks the sharp corners of the exact transformation. In this limit we find

$$E_{\text{disl}} \approx \frac{1}{4\pi} \sum_{i,j} \rho(\mathbf{X}^{(i)}) \rho(\mathbf{X}^{(j)}) \ln \left[\left(X_1^{(i)} - X_1^{(j)} - \frac{b}{2\pi}(\gamma^{(i)} - \gamma^{(j)}) \right)^2 + \left(X_2^{(i)} - X_2^{(j)} + \frac{b}{2\pi} \ln \frac{X^{(i)}}{X^{(j)}} \right)^2 \right] - \sum_i \rho(\mathbf{X}^{(i)})^2 \frac{X_1 b}{2\pi r^2} \quad (33)$$

to lowest order in \mathbf{b} . In this expression $\mathbf{X} = X_1 \hat{\mathbf{e}}_1 + X_2 \hat{\mathbf{e}}_2$, and the dislocation is at the origin. The interaction energy between a charge and a dislocation at the the point \mathbf{x} is in general

$$E_{\text{disc-vort}} \approx \frac{(\mathbf{X} - \mathbf{x}) \times \mathbf{b}(\mathbf{x}) \cdot \hat{\mathbf{e}}_3}{2\pi|\mathbf{X} - \mathbf{x}|^2} \quad (34)$$

to lowest order in b . We see that vortices are attracted or repelled from a dislocation as with a disclination, but the effect is weaker and depends on the orientation of the dislocation as well as its distance. The effect is smallest when \mathbf{b} is perpendicular to the field lines.

A metric with such a dislocation is said to possess *torsion*. Such metrics appear in general relativity with spinning masses.¹⁶

IV. MOTION OF VORTICES IN A CURVED SPACE

We now examine the actual motion of a single vortex in the above two cases. Our problem simplifies considerably because we do not have to worry about vortex-vortex interactions. In order to proceed we need to specify the metric. For the disclination, we choose to work in polar coordinates. The metric can be written

$$g_{ij} = \begin{pmatrix} 1 & 0 \\ 0 & (1 - \frac{\alpha}{2\pi})^2 r^2 \end{pmatrix} \quad (35)$$

For $\alpha = 0$ (or $p = 1$) we recover the flat space metric. Note that the circumference of a circle of radius R in this space is $(2\pi - \alpha)R$. Our Lagrangian in polar coordinates (r, γ) is then

$$\begin{aligned} L &= \frac{1}{2} m_{\text{eff}} g_{ij} \dot{X}_i \dot{X}_j - \frac{\alpha \rho^2}{4\pi^2} \ln X \\ &= \frac{m_{\text{eff}}}{2} \left(\dot{r}^2 + (1 - \frac{\alpha}{2\pi})^2 r^2 \dot{\gamma}^2 \right) - \frac{\rho}{2\pi} (p - 1) \ln r \end{aligned} \quad (36)$$

Solutions of this system can be reduced to quadrature:

$$(\gamma - \gamma_0) = \int_{r_0}^r \frac{dr'}{\sqrt{c_1 - \frac{c_0^2 p^2}{r^2} + \ln r}} \quad (37)$$

where c_1 and c_2 are constants defined by the initial energy and angular momentum. In fig.(4) we show some sample trajectories for vortices propagating ballistically in a junction array with a disclination. Note that for positive disclinations we see a repulsion, and for negative

ones we see an attraction. Also shown are trajectories for fictitious “neutral” vortices that propagate along straightlines. These trajectories show the effect of the vortex-disclination potential.

For the dislocation with Burger’s vector $\mathbf{b} = b \hat{\mathbf{e}}_1$, located at the origin, we choose to work in Cartesian coordinates. We approximate the metric to lowest order in b :

$$g_{ij} = \begin{pmatrix} 1 & -\frac{by}{2\pi r^2} \\ -\frac{by}{2\pi r^2} & 1 + \frac{2bx}{2\pi r^2} \end{pmatrix} \quad (38)$$

In polar coordinates the Lagrangian for the vortex is

$$L = \frac{1}{2}m_{\text{eff}} \left[\dot{r}^2 + r^2\dot{\gamma}^2 + 2b\dot{\gamma}(\dot{r}\sin\gamma r\dot{\gamma}\cos\gamma) \right] - \frac{bV_0}{2\pi} \cos\gamma \quad (39)$$

For $b = 1$ we recover the flat space metric. In fig.(5) we show some sample trajectories for vortices propagating ballistically in a junction array with a dislocation. The trajectory depends upon the relative orientation of the dislocation and the vortex. Also shown are trajectories for “neutral” vortices that propagate along straightlines. These trajectories show the effect of the vortex-dislocation potential.

V. CONCLUSION

In this paper we have shown that the geometry or connectivity of a lattice can have a strong affect on the dynamics of vortices within the lattice. These effects can be seen in the ballistic propagation of vortices. Such experiments have already been performed on regular lattices. We propose that similar experiments could be done with lattices possessing topological defects.

In addition, defects might also change the thermodynamic properties of the lattice. The presence of a postitive disclination acts as an attractive potential for *both* positive and negative vortices, and it alters the interaction between vortices whose separation is comparable to their distance to the defect. These effects may both alter the Kosterlitz-Thouless transition

within the lattice. In addition, it will alter the interactions in the quantum Hall analogs proposed in such arrays.^{15,22}

Since the charge and vortex degrees of freedom are approximately dual,^{13,12} we expect similar results for charge excitations within the lattice. In the limit that we neglect the self-capacitance and the inertial terms in K_i the two exactly dual. The interaction potentials for charge excitations will be identical to those calculated above, since they are both based on finding the inverse of the LB operator. Thus we expect that charge excitations on the lattice will also interact with distortions of the lattice. However, the Coulomb interaction is not strictly two dimensional in real lattices. We expect therefore that interactions with lattice defects will effectively be screened out at distance that depends upon the ratio of the nearest neighbor capacitances to the next-nearest neighbor capacitances.

The motion of charges on twisted lattices also has potential application in tight-binding models of lattices with dislocations, or of carbon nanotubes. In these cases the lattice gives rise to metrics for the kinetic energy that have non-trivial torsion and curvature. These may act as sources of additional scattering or resistance.

Similar interactions between defects in different “order parameters” has been proposed in other systems. This idea is at the heart of the superhexatic state²³ in which the defects that mediate the melting transition interact with superfluid vortex degrees of freedom. A mathematically similar situation arises in the case of tilted smectic liquid crystals.²⁴ This system is composed of a 2D surface of rod-like molecules that orient themselves at a small tilt with respect to the surface normal. The molecules themselves form a liquid crystal, which has disclinations as spatial defects. The $U(1)$ symmetry associated with the orientation of the tilt interacts with the spatial defects in the smectic. The interaction energy between the two (sometimes called “white” and “green” vortices) is analogous to the vortex-disclination energy we have discussed above. It is also amusing to note that these Josephson junction lattices also provide analogs of how charges interact in a 2D gravitational system.

It is quite common to model continuous differential equations by putting them on a mesh. It is usually assumed that the nature of a mesh has no effect on the dynamics of the system,

if the mesh is sufficiently fine. We have shown that topological properties of the mesh can introduce effects in the dynamics of the system being modelled. Care must be taken when using such non-integrable metrics, (*i.e.* those with torsion or curvature).

In the world of superconducting lattices, distance is measured in junctions. This allows the experimenter to create lattices where the excitations move in a curved space, producing several novel effects.

ACKNOWLEDGMENTS

This research was supported by Grant No. DMR-9502555 from the National Science Foundation. Much of this problem was motivated by discussions with A. Stern. We would also like to thank K. Burke, S. M. Girvin, H. T. C. Stoof and M. Wallin for stimulating and helpful discussions.

REFERENCES

¹ R. Fazio and G. Schön, Phys. Rev. B **43**, 5307, (1991).

² A. van Otterlo, R. Fazio and G. Schön, *Physica B* **203** 504 (1994).

³ R. Fazio, A. van Otterlo, and G. Schön, *Euro. Lett.* **25** 453 (1994).

⁴ R. F. Voss and R. A. Webb, Phys. Rev. B **25** 3446 (1992).

⁵ C. J. Lobb, D. W. Abrham, and M. Tinkham, Phys. Rev. B **27** 150 (1983).

⁶ J. E. Mooij, B. J. van Wees L. J. Geerligs, M. Peters, R. Fazio and G. Schön, Phys. Rev. Lett. **65**, 645 (1990).

⁷ W. J. Elioin, J. J. Wachters, L. L. Sohn, and J. E. Mooij, *Physica B* **203** 497 (1994).

⁸ E. Ben-Jacob, K. Mullen, and M. Amman, *Phys. Lett.* **A135**, 390 (1989).

⁹ J. E. Mooij, H. S. J. Van Der Zant, W. J. Elion, in *Proceedings of the 4th International Symposium on Foundations of Quantum Mechanics in the Light of New Technology*, M. Tsukada, S.-I. Kobayashi, S. Kurihara, and S. Nomura, eds. *Japanes J. Appl. Phys*, 72 (1993).

¹⁰ H. S. J. van der Zant, H. A. Rijken, and J. E. Mooij, *J. Low Temp. Phys.* **82** 67 (1991).

¹¹ J. Carini, Phys. Rev. B **38** 63 (1988).

¹² M. P. A. Fisher and D. H. Lee, Phys. Rev. B **39** 2756 (1989).

¹³ R. Fazio, U. Geigenmuller and C. Schon in “Quantum fluctuations in mesoscopic and macroscopic systems,” H. A. Ceredeira, ed., World Scientific (1991).

¹⁴ J. Villain, *J. Physique*, **36** 581 (1975).

¹⁵ A. Stern, Physical Review **B50**, 10092, (1994).

¹⁶ H. Kleinert, *Gauge Fields in Condensed Matter Physics, Vol. 2* (World Scientific, Singa-

pore, 1989).

¹⁷ J. V. José and L. P. Kadanoff, Phys. Rev. B **16**, 1217 (1977).

¹⁸ C. Itzykson and J. M. Drouffe, *Statistical Field Theory, Vol. 2*, (Cambridge University Press, Cambridge England, 1989).

¹⁹ F. Spitzer, *Principles of Random Walk*, (Van Nostrand, Princeton NJ, 1964)

²⁰ *Classical Electricity and Magnetism*”, by W. K. H. Panofsky and M. Phillips, (Addison-Wesley, Reading MA, 1962).

²¹ S. Dreser, R. Jackiw, and G. t’Hooft, *Ann. Phys.* **152** 220 (1984).

²² A. A. Odintsov, and Yu. V. Nazarov, *Physica B* **203** 513 (1994).

²³ K. Mullen, H.T.C. Stoof, M. Wallin, S.M. Girvin, *Phys. Rev. Lett.* **72**, 4013 (1994).

²⁴ D. R. Nelson and B. I. Halperin, *Phys. Rev. B* **21**, 5312 (1980).

FIGURES

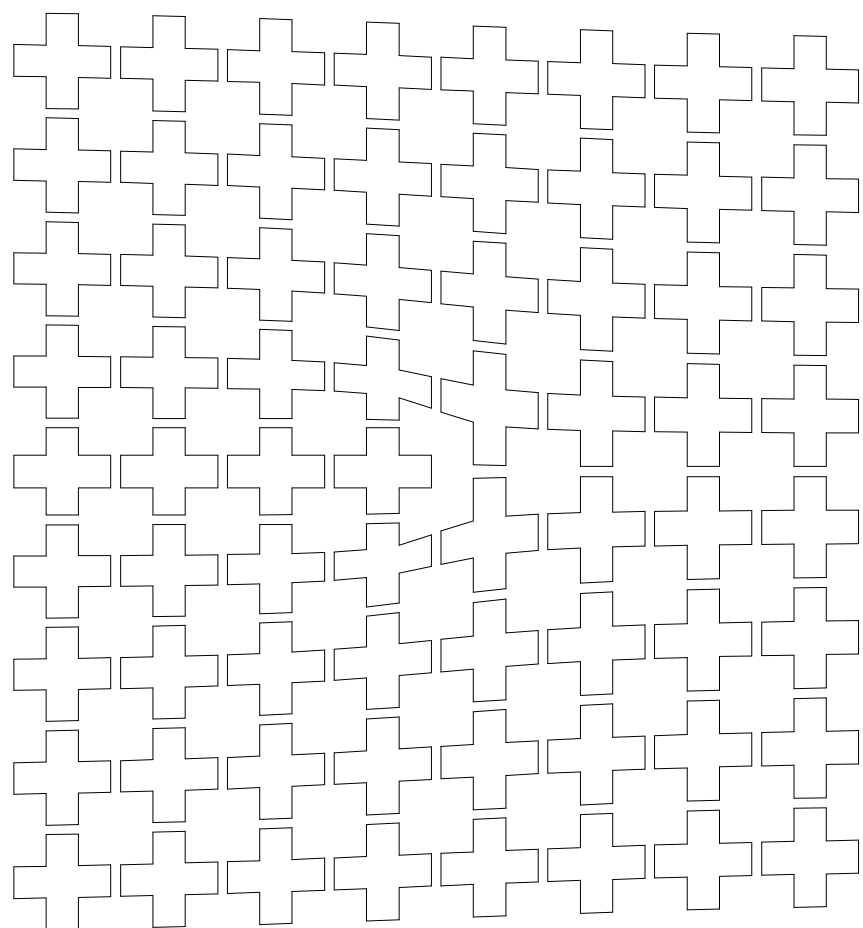
FIG. 1. (a) A square lattice with a dislocation. It can be viewed as a missing horizontal row of islands along the positive x direction, or an inserted row of island along the negative x-axis. (b) A square lattice with a negative disclination. It is formed by removing a 90° wedge from the original square array, and then distorting the lattice so that the open edges meet. Although the system has a center of three-fold symmetry, note that all sites still have four neighbors. To excitations within the lattice it will appear to be a curved space. A positive disclination (not shown) is formed by the insertion of a 90° wedge of material into the lattice. It is also possible to form disclinations in triangular lattices by removing or inserting a 60° wedge of material.

FIG. 2. A schematic representation of a junction lattice where each island is treated as a point. With each lattice point we associate two vectors pointing to the nearest neighbors to the left and above the island. The vectors $\mathbf{u}_{(1)}$ and $\mathbf{u}_{(2)}$ may vary as we move through the lattice.

FIG. 3. To excitations moving within the a junction array, a lattice with a disclination is equivalent to the surface of a cone. If we slice the cone from the tip out to infinity, we can flatten it to the plane. Here we sketch the field lines of a point charge P in such a case, where the wedge of removed material forming the disclination has an opening angle α , and is centered at the origin, O (the tip of the cone). Derivatives of the field are continuous across the cut so by symmetry, the field will approach it tangentially. Because the field lines are “excluded” from the wedge (the shaded area), the field lines are forced closer together, increasing the energy. This results in a repulsive interaction between the point charge and the defect.

FIG. 4. Sample trajectories for a vortex moving in a disclinated lattice, as in fig.(1.b). The disclination is at the origin and has a “charge” or missing angle of $\pi/4$. Show here are trajectories for vortices with an initial velocity v_0 and an impact parameter of r_0 . The dashed line is a trajectory for a “neutral” vortices showing just the effect of geometry. The other lines are trajectories of vortices with interaction energies $\Gamma = E_J/m_{\text{eff}}v_0^2$ of $1/4$, $1/2$, and 1 , from top to bottom. The vortices start at the position $(r_0, -r_0)$. The distances are measured in r_0 .

FIG. 5. Sample trajectories for a vortex moving in a lattice with a dislocation, as in fig.(1.b). The dislocation is a missing row of junctions along the positive x-axis, and is centered at the origin. Show here are trajectories for vortices with an initial velocity v_0 and an impact parameter of r_0 . Plotted are trajectories for “neutral” vortices (dashed line), and vortices with interaction energies $\Gamma = E_J/m_{\text{eff}}v_0^2$ of 0.40 (middle line), and 1.0 (outer line). The distances are measured in r_0 , and $b/r_0 = 0.10$.



(a)

Figure 1a

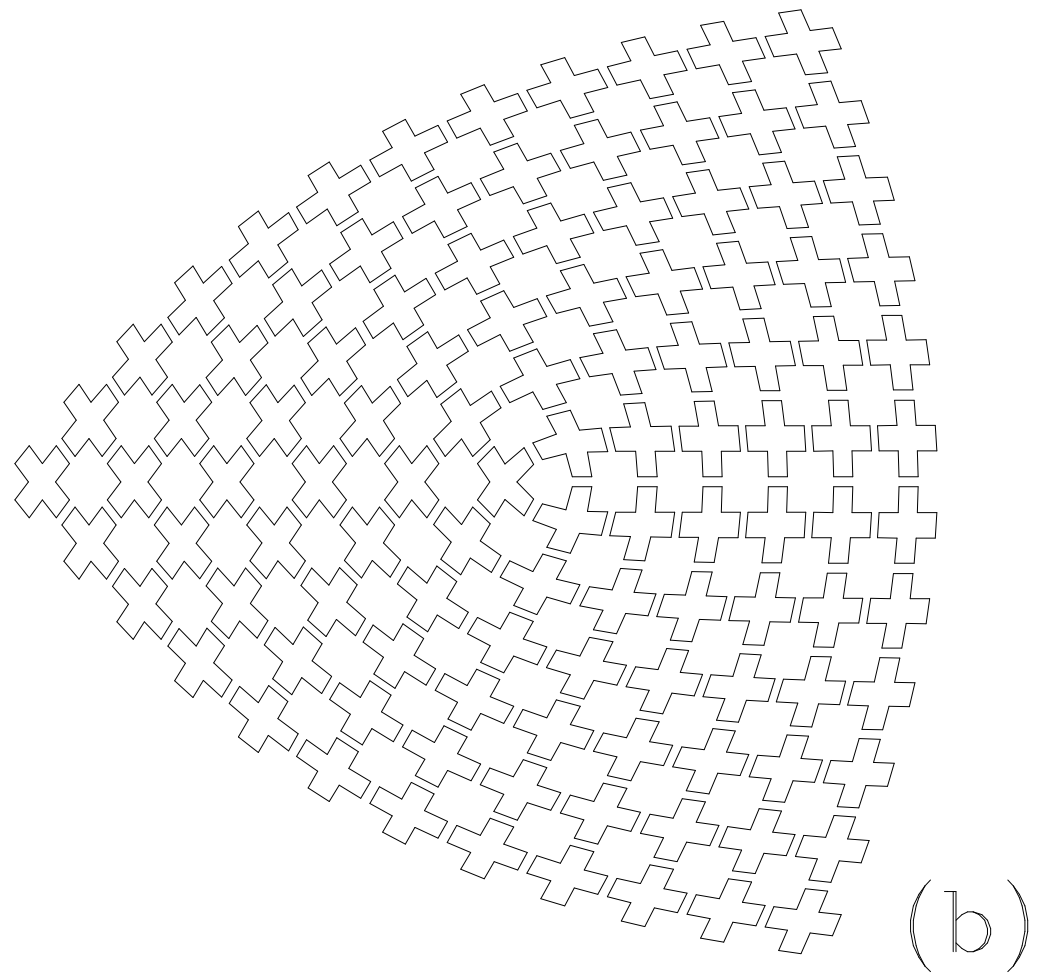


Figure 1b

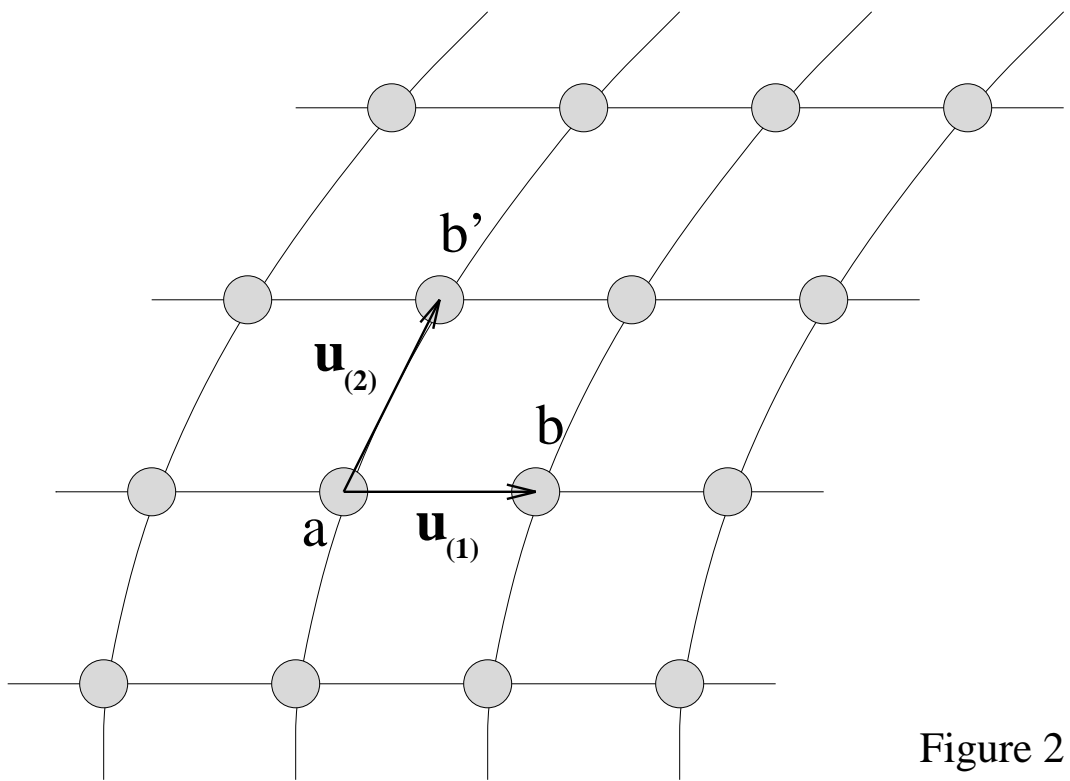


Figure 2

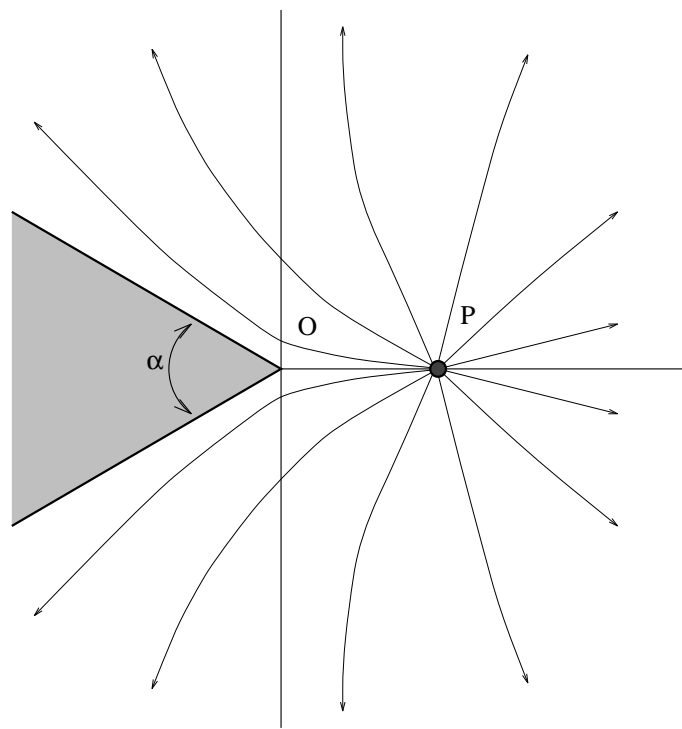


Fig. 3

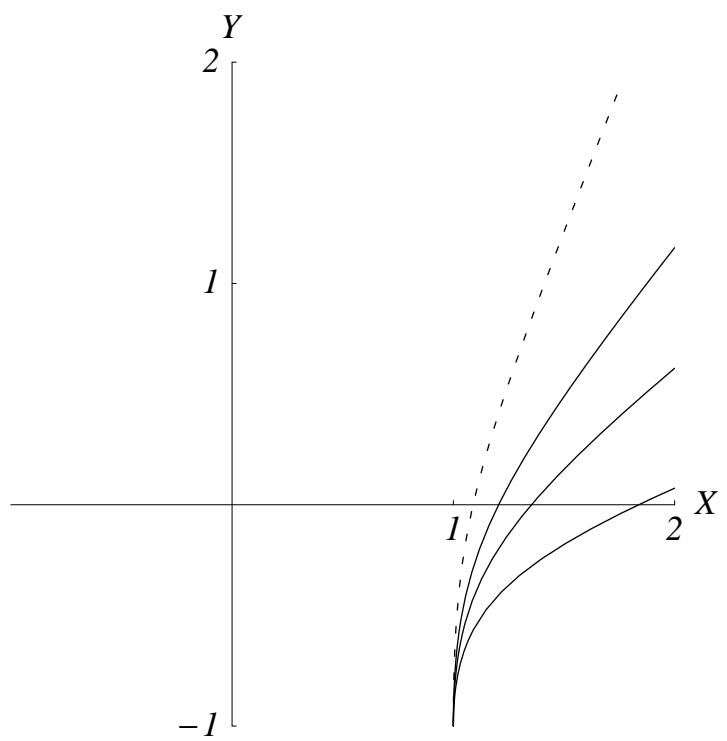


Figure 4

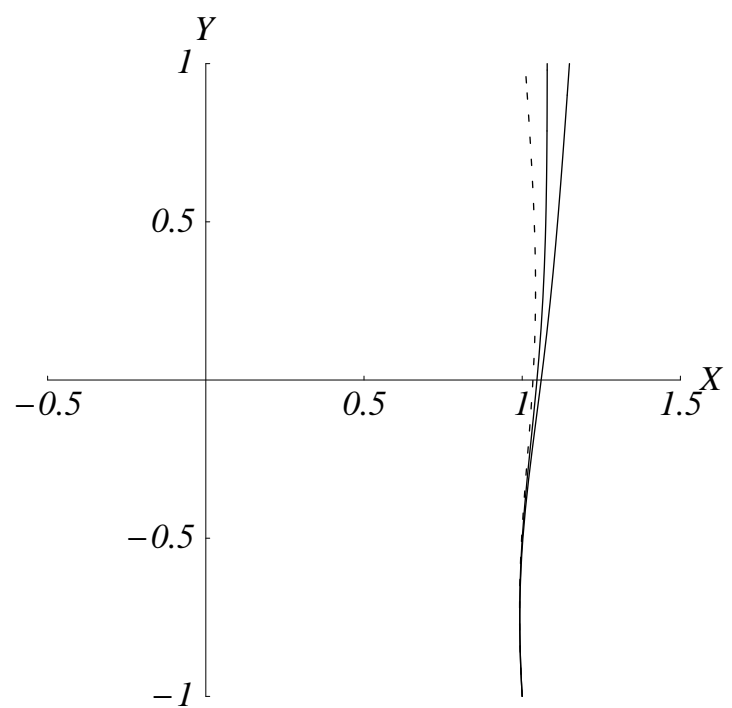


Figure 5